Rotor/Fuselage Vibration Isolation Studies by a Floquet-Harmonic Iteration Technique

R. Sivaramakrishnan* and C. Venkatesan†
Hindustan Aeronautics Limited, Bangalore, India
and
T. K. Varadan‡
Indian Institute of Technology, Madras, India

The equations of motion for the coupled rotor/isolator/fuselage dynamical system are formulated for the prediction of vibrations in helicopters during forward flight. Using a combined Floquet theory/frequency-response technique, the equations are solved to predict the vibratory loads at the various locations of the helicopter. In addition, the influence of the isolator on the hub and blade loads is established.

Nomenclature

A = area
C_{d0} = drag coefficient of blade
C_I = damping constant of isolator system
C_L = lift-curve slope
C_M = aerodynamic moment coefficient of airfoil
C_{MX} = rolling-moment coefficient
C_{MY} = pitching-moment coefficient
C_T = thrust coefficient
D = fuselage drag force
K_I = spring stiffness of isolator system
K_β = root spring stiffness in flap, representing blade stiffness
K_ζ = root spring stiffness in lead lag, representing blade stiffness
K_ϕ = root spring stiffness in torsion, representing blade stiffness
L_1 = distance between pivots
L_2 = distance between outer pivot and isolator mass
M_b = mass of blade
M_F = mass of fuselage
M_H = mass of rotor hub
M_I = isolator mass
M_β = flap moment
M_ζ = lead-lag moment
M_ϕ = torsional moment
N = number of blades
$\bar{P}$ = force vector
$\{q\}$ = generalized coordinate vector
$\bar{Q}$ = moment vector
R = rotor radius
R_F = perturbational motion of fuselage center of gravity
R_H = perturbational motion of hub center
t = time
V_F = forward velocity of helicopter
W = weight of helicopter
α = attitude angle of helicopter
β = flap angle of blade
$\beta_0,\beta_{1C},\beta_{1S}$ = flap angles, collective and cyclic modes, respectively
ζ = lead-lag angle for blade
θ_0 = blade collective pitch
θ_{1C},θ_{1S} = cyclic pitch components of blade
λ = total inflow
λ_i = induced inflow
μ = advance ratio
ρ_A = density of air
ϕ = torsional deformation for blade
ψ = azimuth angle of blade, $=\Omega t$
Ω = rotor frequency
ω = angular velocity of blade

Superscript

$(\dot{})$ = nondimensional time derivative

Introduction

IT is well known that helicopters are plagued with vibrations. The various sources of vibration are the rotors, engine, and transmission system. Of these, the primary source of excitation is the main rotor system, which operates in a complex aerodynamic environment. The rotor blade loads are generated by an interaction of the physical quantities associated with the aerodynamic, inertial, and structural properties of the blade. These vibratory loads are transmitted to different parts of the fuselage through a complicated load path and cause discomfort to the pilot and crew, equipment deterioration, fatigue damage to the structure, and increased maintenance. The adverse effects of these vibratory loads increase with increases in forward speed of the helicopter and also the cumulative fatigue damage to the structure increases with higher utilization of the vehicle. As a result, these vibratory loads restrict the operation and efficiency of the vehicle.

The demand for increasing helicopter usage for passenger transportation and the demand for high-speed maneuverability helicopters for defense have underlined the need for vibration reduction. Vibration reduction can be achieved in a number of ways. In Ref. 1, Loewy has presented an extensive review of the different techniques of vibration reduction in helicopters. Vibration reduction devices are classified into four

Received July 9, 1988; revision received May 25, 1989.

*Aeronautical Engineer, Helicopter Design Bureau.
†Senior Design Engineer, Helicopter Design Bureau. Presently, Assistant Research Engineer, Mechanical Aerospace and Nuclear Engineering, University of California, Los Angeles.
‡Professor, Department of Aeronautical Engineering.

general categories: 1) absorbers,[2-4] 2) blade design optimization,[5-7] 3) isolators,[8-10] and 4) higher harmonic control.[11-15]

Stringent requirements for lower vibrations and penalties in cost and weight have increased the interest in the development of improved vibration reduction methodologies. It is observed that there is hardly a rotorcraft that did not exhibit excessive vibration during initial flight. Sometimes the helicopters have had their flight envelopes reduced because of excessive oscillatory loads.[16] In addition, the vibration level often is very sensitive to even a small variation in the dynamic parameters of the blade. A vibration reduction program based entirely on experiment will be very expensive. However, if the oscillatory loads are predicted accurately, then the cost and time involved in reducing these vibrations to the specified levels can be minimized. Therefore, for the successful design of an efficient vehicle, it becomes essential to develop a theoretical capability for the prediction of oscillatory loads during helicopter flight. A proper treatment of this problem requires a mathematical model representing the dynamics and aerodynamics of the coupled rotor/fuselage system and also a suitable mathematical technique for the analysis of the coupled rotor/fuselage system.

In the past,[17-19] the equations of motion of the coupled rotor/fuselage dynamical system were developed and the vibratory response was predicted by using a harmonic balance technique. However, it must be mentioned that the harmonic balance technique gets quite involved in the algebraic manipulations, particularly for coupled systems. In Ref. 20, Stephens and Peters have critically analyzed the procedures for solving the coupled rotor-body system, namely, the coupled "rotor-body iteration" technique and the "fully coupled equations" approach. Based on an example problem, the authors have shown that the coupled rotor-body iteration technique can sometimes lead to lack of convergence. On the other hand, the fully coupled equations approach does not suffer from the deficiencies of the rotor-body iteration scheme.

In the present paper, a combination of the Floquet theory/frequency-response technique is used to solve the coupled rotor/isolator/fuselage dynamical problem for the prediction of helicopter vibrations. It may be noted that this technique essentially falls under the category of a coupled rotor-body iteration scheme, mentioned in Ref. 20. In employing this technique of combined Floquet theory/frequency response, no approximation is made in the response evaluation of the rotor blade. In this technique, the blade equations are solved in the time domain, whereas the hub/fuselage/isolator response equations are solved algebraically in the frequency domain.

The major objectives of the present study are as follows:

1) Development of the complete set of dynamical equations of motion representing the coupled rotor/isolator/fuselage system in forward flight.

2) Application of a combination of Floquet theory/frequency-response technique for vibration analysis of the helicopter in forward flight.

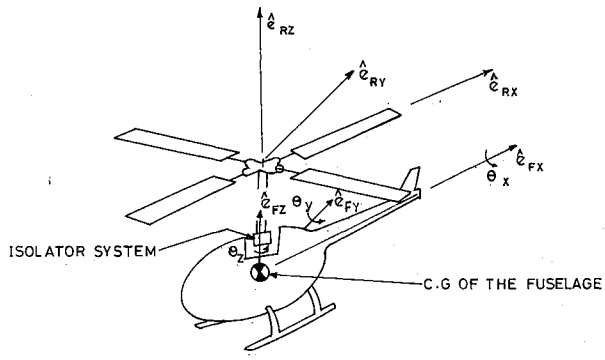

Fig. 1 Model of rotor/isolator/fuselage system.

3) Prediction of the vibratory loads at certain critical locations, such as blade root, rotor hub, fuselage c.g., etc.

4) A fundamental understanding of the effects of the isolator on the blade and fuselage loads.

Equations of Motion

The equations of motion are derived for the coupled rotor/isolator/fuselage dynamical system shown in Figs. 1 and 2. Figure 2 gives the details of the idealized dynamic antiresonant vibration isolation (DAVI) type of vibration reduction device used for the present analysis. The spring and dashpot combination acts as an isolator and the pivoted mass acts as an absorber. The upper mass M_H simulates the rotor hub system and the lower mass M_F simulates the fuselage. The isolator mass M_I displacement is a function of the displacements of upper and lower masses. The important assumptions made in the development of the equations of motion of the coupled rotor/isolator/fuselage system are the following:

1) The blade is assumed to be rigid, with root springs simulating the fundamental frequencies in flap, lag, and torsional degrees of freedom.

2) Fuselage is assumed to be a rigid body.

3) Two-dimensional quasisteady aerodynamics is used for aerodynamic loads determination.

4) Uniform inflow model is used.

The equations of motion of the individual blade are derived in a manner similar to that detailed in Ref. 21. Since a rigid, offset-hinged, spring-restrained model of the blade is used, the equations of motion for the blade are obtained by enforcing moment equilibrium at the root of the blade. The blade equations of motion can be written in symbolic form as

Flap:

$$M_\beta + Q_{I_\beta} + Q_{A_\beta} + Q_{D_\beta} = 0 \tag{1}$$

Lead lag:

$$M_\zeta + Q_{I_\zeta} + Q_{A_\zeta} + Q_{D_\zeta} = 0 \tag{2}$$

Torsion:

$$M_\phi + Q_{I_\phi} + Q_{A_\phi} + Q_{D_\phi} = 0 \tag{3}$$

where M_β, M_ζ, and M_ϕ are the restraining root moments due to the root springs, and Q_I, Q_A, and Q_D are the inertia, aerodynamic, and damping moments due to blade motion.

The blade loads, which are functions of both the blade and the hub motions, contain all harmonics of the rotor rotational frequency. These individual blade loads combine at the rotor hub, resulting in the cancellation of some of the harmonics and addition of other harmonics. As a result, the vibratory hub loads have frequencies that are integer multiples of the blade passage frequency (i.e., $nN\Omega$, where n is the harmonic number $= 1,2,3,\ldots$; N the number of blades; and Ω the rotor speed). These rotor hub loads are used for the development of the coupled rotor hub/isolator/fuselage dynamical equations of motion.

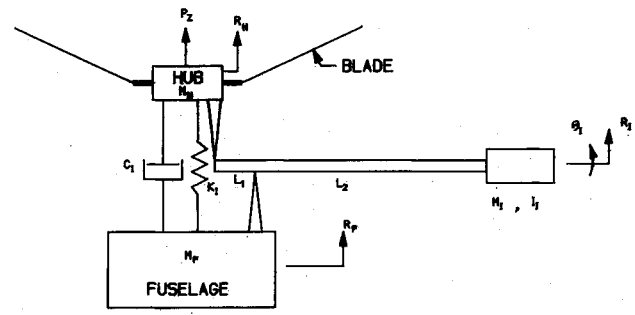

Fig. 2 Rotor hub/isolator/fuselage dynamical model.

With vibration isolation considered only in the vertical direction, the dynamical equations of motion for the coupled rotor hub/isolator/fuselage system can be written as

$$M_H\ddot{R}_H + M_I L_2^2\ddot{R}_H/L_1^2 - M_I L_2(L_1+L_2)\ddot{R}_F/L_1^2 + I_I\ddot{R}_H/L_1^2 - I_I\ddot{R}_F/L_1^2 + C_I(\dot{R}_H-\dot{R}_F) + K_I(R_H-R_F) = P_Z \quad (4)$$

$$M_F\ddot{R}_F + M_I(L_1+L_2)^2\ddot{R}_H/L_1^2 - M_I L_2(L_1+L_2)\ddot{R}_H/L_1^2 + I_I\ddot{R}_F/L_1^2 - I_I\ddot{R}_H/L_1^2 + C_I(\dot{R}_F-\dot{R}_H) + K_I(R_F-R_H) = 0 \quad (5)$$

In Eq. (4), P_Z represents the hub load in the vertical direction; it may be noted that this hub load is a function of fuselage and blade degrees of freedom. Details of the derivation of the equations of motion are available in Ref. 22.

Method of Solution

The coupled rotor/isolator/fuselage dynamical problem is solved in two stages. In the first stage, the trim or equilibrium state of the helicopter is evaluated for a given flight condition; in the second stage, the response of the coupled dynamical system is determined. A brief description of these two stages of the analysis is provided next.

Trim or Equilibrium State Solution of the Vehicle

In the trim analysis, the force and moment equilibrium of the complete vehicle together with the moment equilibrium of the individual blade about its root in lag, flap, and torsion are enforced. This type of trim usually is denoted as propulsive trim. A propulsive trim analysis simulates the free-flight condition of the helicopter and involves the calculation of blade control settings as well as the vehicle attitude for a prescribed flight condition.

Figure 3 shows the various forces and moments acting on the vehicle. The trim solution is evaluated from the vehicle and blade equilibrium equations, which are as follows:

Vehicle equilibrium:

$$P_Z - W\cos\alpha - D\sin\alpha = 0 \quad \text{(vertical direction)} \quad (6)$$

$$P_X + D\cos\alpha - W\sin\alpha = 0 \quad \text{(longitudinal direction)} \quad (7)$$

$$Q_{YF} + C_{MY}\rho_A A V^2 R/2 = 0 \quad \text{(pitch moment about c.g. of the vehicle)} \quad (8)$$

$$Q_{XF} + C_{MX}\rho_A A V^2 R/2 = 0 \quad \text{(roll moment about c.g. of the vehicle)} \quad (9)$$

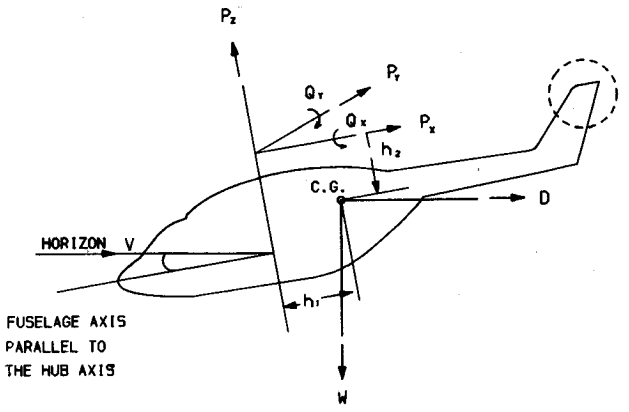

Fig. 3 Longitudinal forces and moments for trim analysis.

Blade equilibrium:

$$\int_0^{2\pi} (\text{flapping moment equation})\, d\psi = 0 \quad (10)$$

$$\int_0^{2\pi} (\text{flapping moment equation})\cos\psi\, d\psi = 0 \quad (11)$$

$$\int_0^{2\pi} (\text{flapping moment equation})\sin\psi\, d\psi = 0 \quad (12)$$

The total inflow λ, through the rotor disk, is given as[23]

$$\lambda = \lambda_i + \mu\tan\alpha \quad (13)$$

where λ_i is the induced inflow given by

$$\lambda_i = C_T/\left[2\sqrt{\mu^2 + (\mu\tan\alpha + \lambda_i)^2}\right] \quad (14)$$

For a given helicopter weight and a given forward speed (advance ratio, μ), the set of Eqs. (6-14) is solved by an iterative numerical method to obtain the different trim parameters, such as the pitch settings θ_0, θ_{1C}, and θ_{1S} of the blade, the vehicle pitch attitude α, and the inflow ratio λ. The various steps involved in the iterative procedure are outlined next.

For a given set of parameters of the vehicle, the rotor and the flight conditions, initially θ_0, θ_{1C}, θ_{1S} (the blade pitch settings), and α (the vehicle attitude), are assumed.

1) From the inflow equations [Eqs. (13) and (14)], the inflow ratio λ is computed by an iterative numerical method.

2) Using the blade flap equilibrium equations [Eqs. (10-12)], the blade flapping coefficients β_0, β_{1C}, and β_{1S} are evaluated.

3) Substituting the values of λ, β_0, β_{1C}, β_{1S}, and α in the vehicle vertical equilibrium equation [Eq. (6)] and also in the vehicle pitching and rolling moment equilibrium equations [Eqs. (8) and (9)], the blade pitch settings θ_0, θ_{1C}, and θ_{1S} are determined.

4) Using the vehicle longitudinal equilibrium equation [Eq. (7)], the attitude angle, α, of the vehicle is calculated, by an iterative numerical technique.

Steps 1-4 are repeated until convergence is achieved for the independent trim parameters θ_0, θ_{1C}, θ_{1S}, and α to the desired level of accuracy. It may be noted that, in the trim procedure, only flap degree of freedom of the blade is considered and also only the fundamental harmonic (first harmonic) components of the flap angle are included. The implication and limitations of using only the fundamental harmonics of flap motion will be explained in the section providing the results.

Response Analysis

The dynamical equations of motion for the response analysis consist of two sets of equations. One involving the blade motion and the other dealing with the hub/fuselage motions. The equations of motion follow.

Blade motion:

$$[M]_q\{\ddot{q}\} + [C]_q\{\dot{q}\} + [K]_q\{q\} = \{Q\} \quad (15)$$

Here $[C]_q$ and $[K]_q$ are functions of time.

Hub/isolator/fuselage:

$$[M]_F\begin{Bmatrix}\ddot{R}_H\\ \ddot{R}_F\end{Bmatrix} + [C]_F\begin{Bmatrix}\dot{R}_H\\ \dot{R}_F\end{Bmatrix} + [K]_F\begin{Bmatrix}R_H\\ R_F\end{Bmatrix} = \begin{Bmatrix}P_Z\\ 0\end{Bmatrix} \quad (16)$$

In the blade equation given by Eq. (15), the forcing vector $\{Q\}$ is a function of the control setting angles, θ_0, θ_{1C}, and θ_{1S}, advance ratio μ, inflow ratio λ, the hub motion $\ddot{R}_H$ and $\dot{R}_H$, and the azimuthal angle ψ, and in the hub/isolator/fuselage equation given by Eq. (16), the forcing vector $\{P_Z\ 0\}$ is a function of the blade motion $\ddot{\beta}$,$\dot{\beta}$, control setting angles θ_0, θ_{1C},

θ_{1S}, inflow ratio λ, advance ratio μ, the hub motion $\ddot{R}_H, R_H$, and the azimuthal angle ψ. Since the blade equations are in a rotating frame, they are differential equations with periodic coefficients. The hub/isolator/fuselage equations are in a nonrotating inertial frame; hence, they are differential equations with constant coefficients. The solution method used for solving the set of equations is a combined Floquet theory/frequency-response technique. In this technique, the blade response is evaluated using Floquet theory and the hub/fuselage equations are solved using the frequency-response technique. The iterative procedure involved in this type of technique is that, first, by assuming the fuselage motion to be zero, the blade equations are solved for their response. Using the hub loads corresponding to this response, the fuselage equations are solved for fuselage/hub response. With this new set of hub response, the blade equations are again solved. This procedure is continued until convergence is achieved. The details of the procedure followed for response analysis are explained next.

The method of solution for the blade equations, using Floquet theory, adopted in this paper, essentially follows the procedure of Ref. 24. Rewriting the blade equation given by Eq. (15) in the state-variable form, one may get

$$\{\dot{q}(\psi)\} = [L(\psi)]\{q(\psi)\} + \{Q(\psi)\} \tag{17}$$

where

$$\{q(\psi)\} = \begin{Bmatrix} \dot{\beta} \\ \dot{\zeta} \\ \dot{\phi} \\ \beta \\ \zeta \\ \phi \end{Bmatrix}$$

and

$$[L(\psi)] = \begin{bmatrix} -[M]_q^{-1}[C]_q & -[M]_q^{-1}[K]_q \\ [I] & [0] \end{bmatrix}$$

Since the system is periodic (of period 2π)

$$\{Q(\psi)\} = \{Q(\psi+2\pi)\} \quad \text{and} \quad [L(\psi)] = [L(\psi+2\pi)]$$

From Floquet-Liapunov theory, the unique periodic solution of Eq. (17) is given by

$$\{q(\psi)\} = [\Phi(\psi)]\left\langle \int_0^{\psi} [\Phi(s)]^{-1}\{Q(s)\}\,ds \times \left\{[I] - [\Phi(2\pi)\right\}^{-1}[\Phi(2\pi)] \int_0^{2\pi} [\Phi(s)]^{-1}\{Q(s)\}\,ds \right\rangle \tag{18}$$

The general solution[25] for any nonhomogeneous equation, such as Eq. (17), can be written as

$$\{q(\psi)\} = [\Phi(\psi)]\{q(0)\} + [\Phi(\psi)] \int_0^{\psi} [\Phi(s)]^{-1}\{Q(s)\}\,ds \tag{19}$$

In Eqs. (18) and (19), $[\Phi(\psi)]$ is the transition matrix defined by

$$[\dot{\Phi}(\psi)] = [L(\psi)][\Phi(\psi)]$$

and

$$[\Phi(0)] = [I]$$

On comparison of Eqs. (18) and (19), it is clear that Eq. (18) corresponds to the general solution of the nonhomogeneous equation [Eq. (15)], with the initial condition

$$\{q(0)\} = \left\{[I] - [\Phi(2\pi)]\right\}^{-1}[\Phi(2\pi)] \int_0^{2\pi} [\Phi(s)]^{-1}\{Q(s)\}\,ds \tag{20}$$

The procedure adopted for the evaluation of the periodic steady-state solution of the blade equation is explained in Ref. 24, which is provided below for convenience.

1) The initial condition $\{q(0)\}$, given by Eq. (20), is first evaluated using the transition matrix at different instants over a complete cycle (2π) and the transition matrix at the end of the cycle $[\Phi(2\pi)]$. This matrix is evaluated using the approximate, semianalytical method[26] (Hsu's method), based on the fourth-order approximation of the matrix exponential. For evaluation of the initial condition, the complete cycle is divided into 52 equal intervals and the integration is done by an ordinary summation.

2) With the initial condition $\{q(0)\}$, computed as described in step 1, the blade response equations given by Eq. (17) are integrated numerically using a fourth-order Runge-Kutta scheme. The integration is performed with a constant step size that is also identical to the step size used in evaluating the transition matrix.

3) Convergence of the method is checked by comparing the response obtained in subsequent revolutions with the initial conditions, i.e., compare $\{q(\psi=0)\}$ with $\{q(\psi=2\pi)\}$, $\{q(\psi=4\pi)\}$, and $\{q(\psi=6\pi)\}$.

4) After evaluating the blade response, the hub and fuselage equations given by Eq. (16) are solved by frequency-response analysis in the following manner.

Assuming the exciting force P_Z to be of the form

$$P_Z = \tilde{P}_Z e^{i\omega t} \tag{21}$$

where $\tilde{P}_Z$ is a constant, the response solution for Eq. (16) can be written as

$$\begin{Bmatrix} R_H \\ R_F \end{Bmatrix} = \begin{Bmatrix} \tilde{R}_H \\ \tilde{R}_F \end{Bmatrix} e^{i\omega t} \tag{22}$$

where R_H and R_F are complex quantities.

Substituting Eqs. (21) and (22) into Eq. (16), the hub and fuselage response may be written as

$$\begin{Bmatrix} R_H/\tilde{P}_Z \\ R_F/\tilde{P}_Z \end{Bmatrix} = \begin{Bmatrix} \text{MOD}_{HN} & e^{i(\omega t+\phi_H)} \\ \text{MOD}_{FN} & e^{i(\omega t+\phi_F)} \end{Bmatrix} \tag{23}$$

where the moduli

$$\text{MOD}_{HN} = \frac{1}{\omega^2}\left[\left\{K_I - \omega^2\langle M_F + M_I(I+L_2/L_1)^2 + I_I/L_1^2\rangle\right\}^2 + \{C_I\omega\}^2 \Big/ \left[\left\{\omega^2\langle M_F M_H + M_H\left\{M_I(I+L_2/L_1)^2 + I_I/L_1^2\right\} + M_F\left\{M_I(L_2/L_1)^2 + I_I/L_1^2\right\} + M_I I_I/L_1^2\rangle - K_I\langle M_F + M_H + M_I\rangle\right\}^2 + \left\{-C_I\omega\langle M_H + M_F + M_I\rangle\right\}^2\right]\right]^{1/2} \tag{24}$$

$$\text{MOD}_{FN} = \frac{1}{\omega^2}\left[\left\{\omega^2\langle M_I L_2/L_1(I+L_2/L_1) + I_I/L_1^2 - K_I\right\}^2 - \{C_I\omega\}^2 \Big/ \left[\left\{\omega^2\langle M_H M_F + M_H\left\{M_I(I+L_2/L_1)^2 + I_I/L_1^2\right\} + M_F\left\{M_I(L_2/L_1)^2 + I_I/L_1^2\right\} + M_I I_I/L_1^2\rangle - K_I\langle M_H + M_F + M_I\rangle\right\}^2 + \left\{-C_I\omega\langle M_H + M_F + M_I\rangle\right\}^2\right]\right]^{1/2} \tag{25}$$

and the respective phase differences are given as

$$\phi_H = \phi_1 - \phi \quad \text{and} \quad \phi_F = \phi_2 - \phi$$

$$\tan\phi = -C_I\omega\langle M_F + M_H + M_I\rangle \Big/ \Big[\omega^2\langle M_H M_F + M_H\{M_I(I + L_2/L_1)^2 + I_I/L_1^2\} + M_F\{M_I(L_2/L_1)^2 + I_I/L_1^2\} + M_I I_I/L_1^2\rangle - K_I\langle M_H + M_F + M_I\rangle\Big]$$

$$\tan\phi_1 = C_I\omega \Big/ \Big[K_I - \omega^2\langle M_F + M_I(I + L_2/L_1)^2 + I_I/L_1^2\rangle\Big]$$

$$\tan\phi_2 = C_I\omega \Big/ \Big[-\{\omega^2\langle M_I L_2/L_1(I + L_2/L_1) + I_I/L_1^2\rangle - K_I\}\Big]$$

Treating the sine and cosine components of the excitation force as acting separately, from Eq. (23), one can write the velocity and acceleration components of the hub and fuselage as

$$\dot{R}_H = \mathrm{MOD}_{HN}(-\tilde{P}_{NZC}\sin N\psi + \tilde{P}_{NZS}\cos N\psi)N + \mathrm{MOD}_{H2N}(-\tilde{P}_{2NZC}\sin 2N\psi + \tilde{P}_{2NZS}\cos 2N\psi)2N \quad (26)$$

$$\dot{R}_F = \mathrm{MOD}_{FN}(-\tilde{P}_{NZC}\sin N\psi + \tilde{P}_{NZS}\cos N\psi)N + \mathrm{MOD}_{F2N}(-\tilde{P}_{2NZC}\sin 2N\psi + \tilde{P}_{2NZS}\cos 2N\psi)2N \quad (27)$$

$$\ddot{R}_H = \mathrm{MOD}_{HN}(-\tilde{P}_{NZC}\cos N\psi - \tilde{P}_{NZS}\sin N\psi)(N)^2 + \mathrm{MOD}_{H2N}(-\tilde{P}_{2NZC}\cos 2N\psi - \tilde{P}_{2NZS}\sin 2N\psi)(2N)^2 \quad (28)$$

$$\ddot{R}_F = \mathrm{MOD}_{FN}(-\tilde{P}_{NZC}\cos N\psi - \tilde{P}_{NZS}\sin N\psi)(N)^2 + \mathrm{MOD}_{F2N}(-\tilde{P}_{2NZC}\cos 2N\psi - \tilde{P}_{2NZS}\sin 2N\psi)(2N)^2 \quad (29)$$

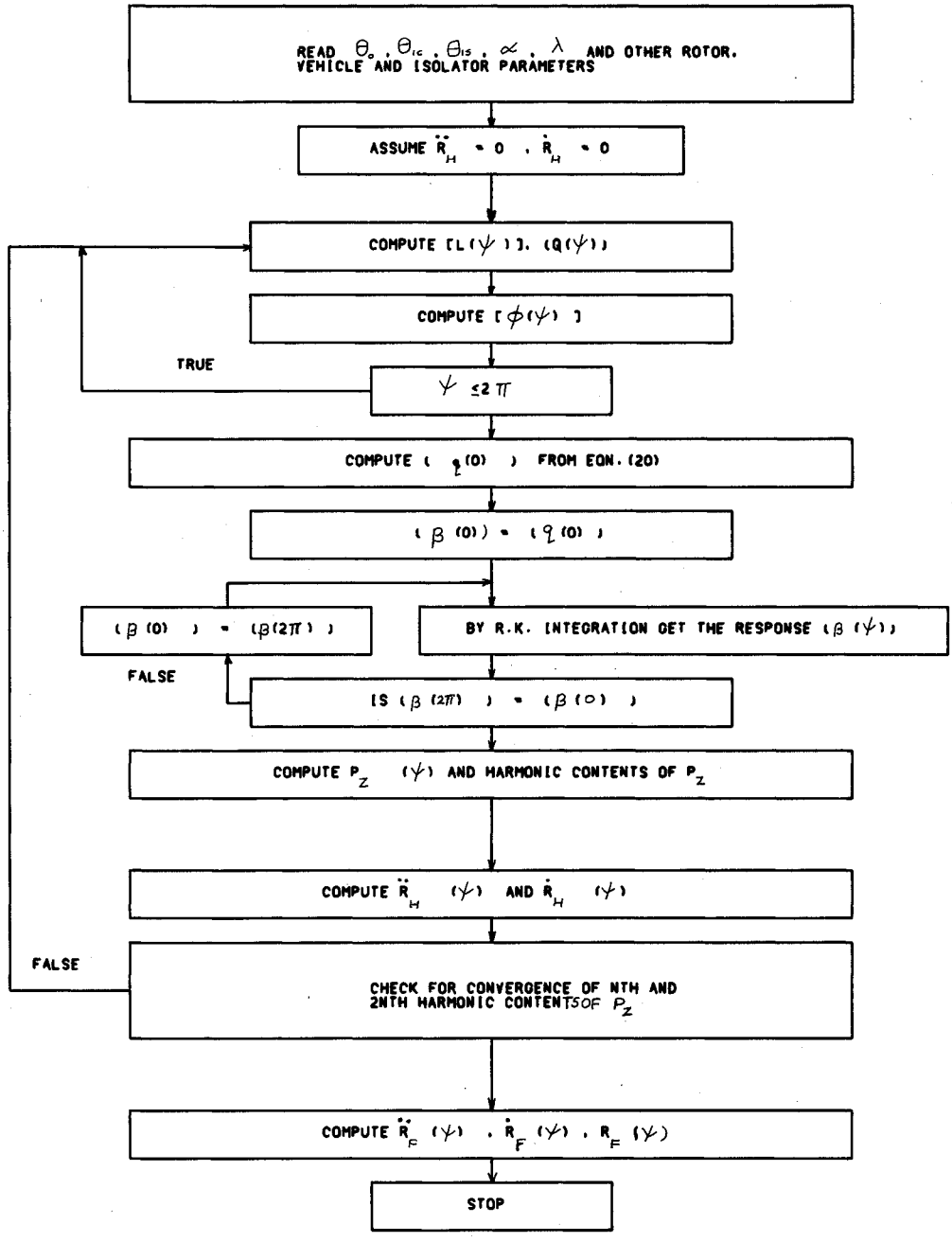

Fig. 4 Flowchart for evaluation of response.

where MOD_{HN} and MOD_{H2N} are given by Eq. (24) for $\omega = N\Omega$ and $\omega = 2N\Omega$, respectively (N being the number of blades). MOD_{FN} and MOD_{F2N} are given by Eq. (26) for $\omega = N\Omega$ and $\omega = 2N\Omega$, respectively. $\tilde{P}_{NZC}$, $\tilde{P}_{NZS}$, $\tilde{P}_{2NZC}$, and $\tilde{P}_{2NZS}$ are the Nth and $(2N)$th harmonic contents of the excitation force P_Z acting at the center of the hub. Using the solution of flap response of the blade, calculated as explained in step 3, the hub vertical force P_Z over one revolution, due to all the blades, is evaluated. By performing a Fourier series expansion of P_Z, the Nth and $(2N)$th harmonic components $\tilde{P}_{NZC}$, $\tilde{P}_{NZS}$, $\tilde{P}_{2NZC}$, and $\tilde{P}_{2NZS}$ are obtained. With these harmonic contents, the time response of the hub and fuselage is determined using Eqs. (26–29). With these new values of the response of the hub and fuselage, the solution procedure is repeated from step 1. Convergence is checked for the Nth and $(2N)$th harmonic contents of the excitation force P_Z. If the convergence is not reached, with the new values of the hub response, steps 1–4 are repeated. A flowchart explaining the different steps involved in the evaluation of the response is given in Fig. 4.

In the above procedure, it is important to recognize that we are not really solving the hub and fuselage equation in the time domain. Rather the solution in the time domain is evaluated using the frequency-response expression. This type of combined Floquet theory/frequency-response technique of solving the coupled rotor/isolator/fuselage/dynamical problem has not been tried and presented in the literature. The main advantage of this new technique is reduced computation time in solving for the response of the hub and fuselage.

Regarding the solution procedure for the response analysis, it is important to mention here that in Ref. 20 the authors have indicated that the rotor-body iteration scheme (as adopted in this paper) can sometimes lead to a lack of convergence problems. The criterion for convergence is shown to be that the ratio of hub mass to pylon mass (in the present case, the fuselage mass) must be small compared to unity. Since this criterion is satisfied for the data considered in the present study, the coupled rotor/isolator/fuselage analysis did not have any convergence problem.

It is also important to note that, as mentioned in Ref. 20, one can adopt a fully coupled rotor-body solution technique for this problem. There are two possible ways of solving the fully coupled rotor-body equation: the harmonic balance method[19] and application of Floquet theory. In applying Floquet theory, one must be careful to eliminate the singularities in the matrix $[I - \Phi(2\pi)]$ in Eq. (18), which appear due to the presence of rigid-body modes of fuselage. Otherwise, Floquet theory solution for the response problem will diverge.

Results and Discussions

Vibration analysis is carried out for a four-bladed rotor with zero precone. The chordwise offsets of the c.g. and the aerodynamic center from the elastic axis of the blade are zero. The fuselage c.g. lies on the shaft axis.

The various data used in the present analysis are provided in Table 1.

The vibratory loads at various locations in the helicopter are evaluated using the dynamical equations of motion of the coupled rotor/isolator/fuselage system. The solution procedure adopted is a combination of Floquet theory and frequency-response technique. The time-varying loads on the helicopter are obtained for various forward speeds. Two sets of cases are analyzed, and they correspond to 1) a system with an isolator and 2) a system without an isolator. Based on these studies, the influence of the isolator on the loads is established.

Trim Analysis

The results of the propulsive trim analysis are presented in Fig. 5. The various trim parameters considered are the inflow ratio (λ), the collective and cyclic pitch angles (θ_0, θ_{1C}, θ_{1S}), and the fuselage attitude (α). The collective pitch angle of the blade decreases initially and then increases with increases in forward speed (μ) of the helicopter. The initial reduction in θ_0 is due to the increased mass flow through the rotor disk, which, in turn, reduces the power required for the flight. However, at high forward speeds, although there is still an increase in the mass flow rate, the power required to overcome the vehicle parasite drag increases, which leads to an increase in the collective pitch setting (θ_0). The total inflow ratio (λ) also follows a similar trend. The cyclic pitch angles θ_{1C} and θ_{1S} increase with increases in forward speed, since they have to compensate for the increasing roll and pitch moments, respectively. As a result of increases in vehicle drag and pitching moment with forward speed, the fuselage attitude (α) also increases monotonically.

Table 1 The various data used in this study are provided below in nondimensional form

Lift-curve slope	a	2π
Blade profile drag coefficient	C_{d0}	0.0079
Fuselage aerodynamic coefficients	C_{MX}	0.0
	C_{MY}	0.0
Density of air	ρ_A	1.225 kg/m
Solidity ratio	σ	0.1
Number of blades	N	4
Lock number	γ	12
Blade flap frequency (rotating)		1.1
Equivalent flat-plate area of fuselage	A/R^2	0.037
Height of rotor hub above c.g. of the helicopter	h_2/R	0.426
Offset between c.g. of the helicopter and rotor hub	h_1/R	0.0
Isolator pivot distance	L_1/L_2	0.08
Isolator spring stiffness	$K_I/M_b\Omega^2$	130
Weight of the helicopter	$\frac{W}{\rho\pi R^2(\Omega R)^2}$	0.0032

Response Analysis

The results for the response analysis are presented in Figs. 6–11. It can be seen from Fig. 6 that the behavior of the flap response evaluated from trim analysis and from response analysis matches very well for forward speeds, $\mu \leq 0.2$. (Note: In trim analysis, only the first harmonic contents of the flap response are considered.) For forward speed $\mu = 0.3$, it is found that there is a marked difference between the flap response behavior obtained in trim analysis and that predicted in the response analysis. It may be noted that, for proper treatment of the problem, the blade response obtained from trim analysis

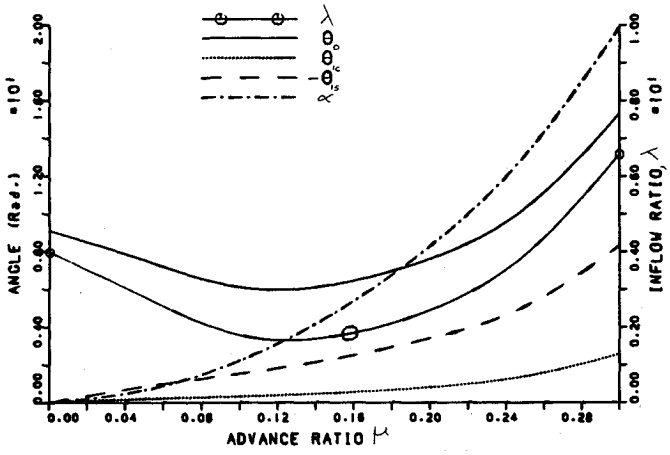

Fig. 5 Variation of trim parameters with advance ratio.

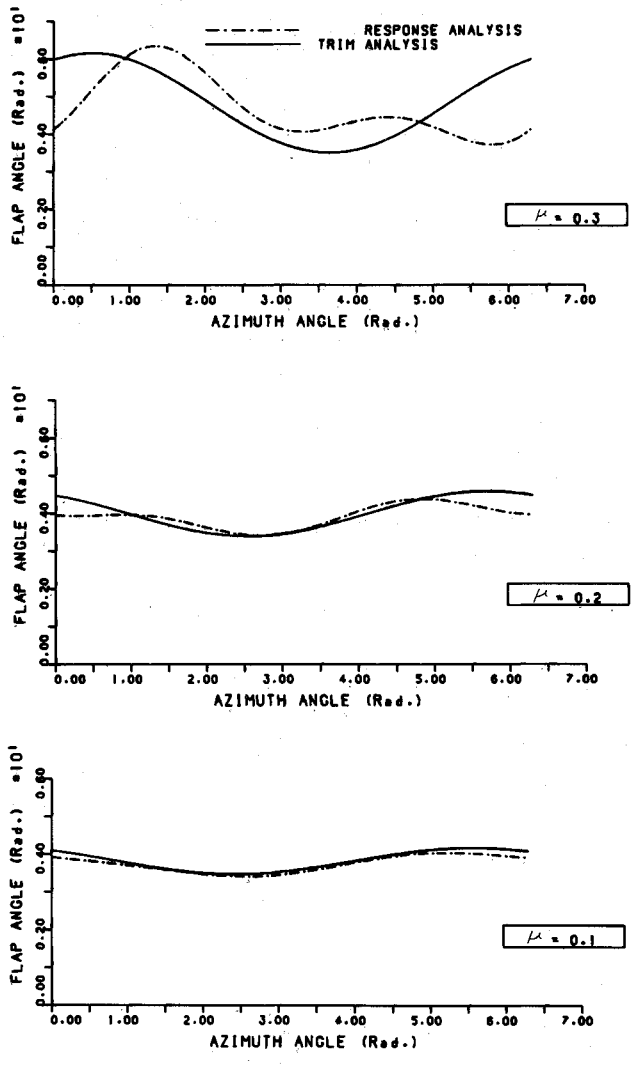

Fig. 6 Comparison of flap response from trim analysis and response analysis.

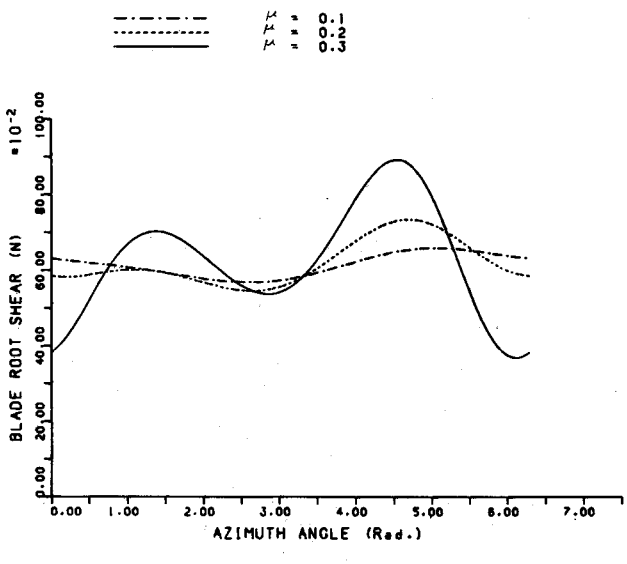

Fig. 7 Variation of blade root shear at different advance ratios.

and response analysis must be the same. Based on the present results, it may be concluded that, for low forward speeds ($\mu \leq 0.2$) an assumption of flap response having only the first harmonic contents is a very good approximation. However, for high speeds, higher harmonics of the flap response must be included, even in trim analysis.

Figure 7 shows the variation of the blade vertical root shear at different forward speeds. At $\mu = 0.1$, the variation seems to be primarily first harmonic; however, as the forward speed increases, the contribution from higher harmonic contents becomes significant. The harmonic contents of the blade vertical root shear are shown in Fig. 8. It is observed that, at $\mu = 0.3$, the second harmonic content becomes greater than the first harmonic content.

Figure 9 presents the variation of time-dependent hub vertical load at different forward speeds. It can be observed that the hub vertical load increases significantly with increases in forward speed. The amplitude of the load increases by about 800% for a forward speed change from $\mu = 0.1$ to 0.3.

The influence of the isolator on the vibratory response of the fuselage and hub is shown in Figs. 10 and 11. In these figures,

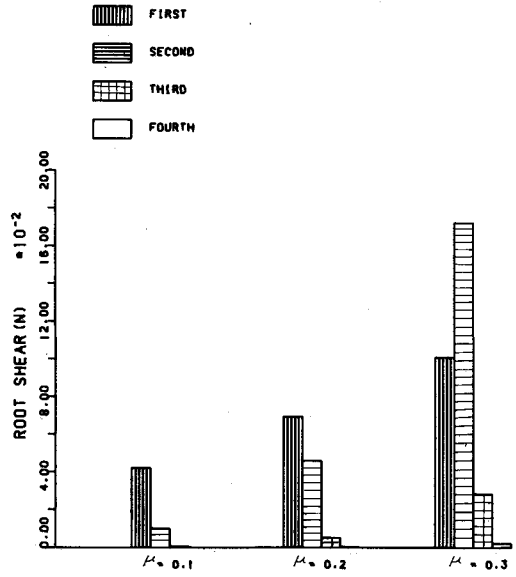

Fig. 8 Harmonics of blade root shear at different advance ratios.

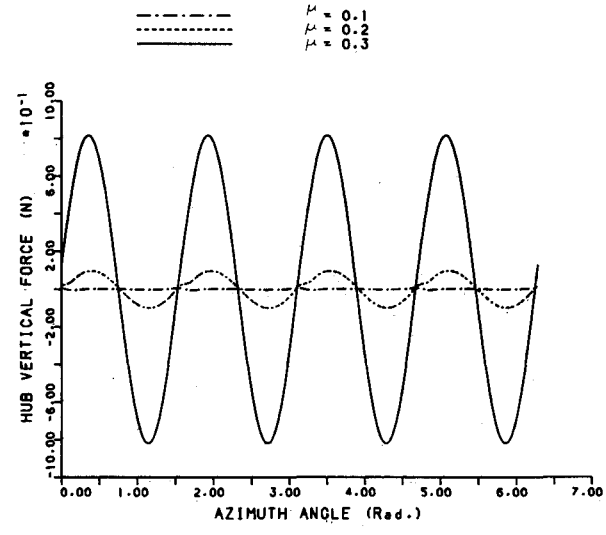

Fig. 9 Variation of hub vertical force at different advance ratios.

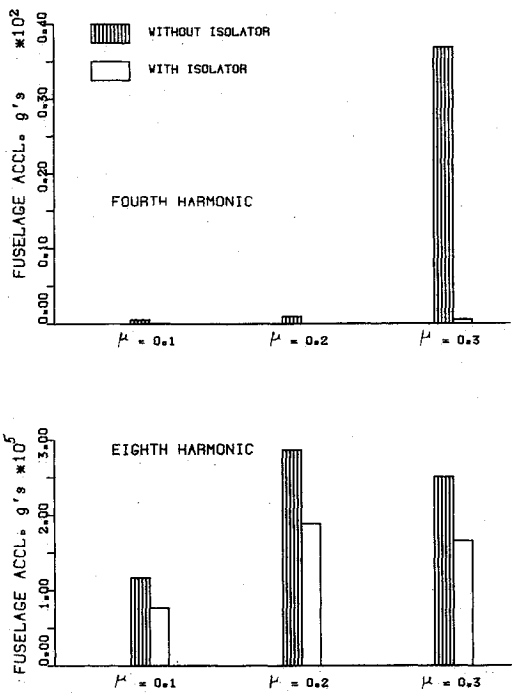

Fig. 10 Influence of isolator on harmonics of fuselage response.

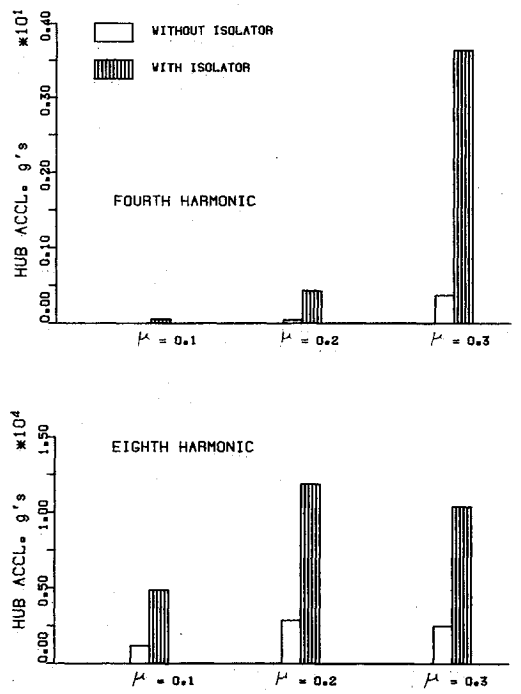

Fig. 11 Influence of isolator on harmonics of hub response.

the fourth and eighth harmonic contents of the response of the hub and fuselage are indicated for two cases: without an isolator and with an isolator. It can be seen from Fig. 10 that the g levels at the fuselage c.g. increase with increases in forward speed. With the inclusion of the isolator, the fourth harmonic content of the fuselage response is almost eliminated. In addition, the eighth harmonic content is also reduced by about 30%. It is observed that the eighth harmonic content of the fuselage response is two orders lower than the fourth harmonic content.

Figure 11 shows the harmonic contents of the hub acceleration. It can be seen from this figure that the inclusion of the isolator increases significantly the harmonic contents of the acceleration. For example, at $\mu = 0.3$, with the inclusion of the isolator, the fourth harmonic content is increased approximately eightfold and the eighth harmonic content by about fourfold.

Concluding Remarks

In the present analysis on the prediction and reduction of vibration in helicopters, the complete set of dynamical equations of motion for the coupled rotor/isolator/fuselage system is derived. A combination of Floquet theory and the frequency-response technique is applied for the solution of the coupled rotor/isolator/fuselage problem. The effect of the inclusion of the isolator on the various loads of the system is studied. A summary of important observations of the present study is as follows:

1) A combination of Floquet theory and the frequency-response technique is applied successfully for solving the coupled rotor/isolator/fuselage dynamical problem. In this technique, the rotor blade equations having periodic coefficients are solved by Floquet theory in the time domain, whereas the hub/isolator/fuselage response equations are solved algebraically using the frequency-response method.

2) In trim analysis, for low forward speeds ($\mu \leq 0.2$), the assumption of a flap response, consisting of only first harmonic contents, is a very good approximation. However, for high forward speeds, for a proper treatment of the problem, higher harmonic contents of the flap response must be considered in trim analysis.

3) The blade loads and blade response increase with increases in forward speed of the helicopter. With increases in forward speed, the second harmonic content of the blade vertical root shear becomes more and more significant, and it is observed that at $\mu = 0.3$ the second harmonic content is more than the first harmonic content.

4) The hub loads increase significantly with increases in forward speed. When the forward speed of the helicopter is increased from $\mu = 0.1$ to 0.3, the peak-to-peak variation of the time-dependent hub vertical load is increased by about 800%.

5) Inclusion of an isolator between the hub and the fuselage reduces the fuselage vibratory loads and increases the hub loads significantly.

Acknowledgment

The authors wish to thank the reviewer for the critical comments that helped in improving the quality of this paper.

References

[1]Loewy, R. G., "Helicopter Vibrations—A Technological Perspective," *Journal of the American Helicopter Society,* Vol. 29, No. 4, Oct. 1984, pp. 4-30.

[2]Hamouda, M. H. and Pierce, G. A., "Helicopter Vibration Suppression Using Simple Pendulum Absorbers on the Rotor Blade," *Journal of the American Helicopter Society,* Vol. 29, No. 3, July 1984, pp. 19-29.

[3]Viswanathan, S. P. and McClure, R. D., "Analytical and Experimental Investigation of a Bearingless Hub Absorber," *Journal of the American Helicopter Society,* Vol. 28, No. 3, July 1983, pp. 47-55.

[4]Taylor, R. B. and Teare, P. A., "Helicopter Vibration Reduction with Pendulum Absorbers," *Proceedings of the 30th Annual National Forum of the American Helicopter Society,* Washington, DC, May 1974.

[5]Blackwell, R. H., "Blade Design for Reduced Helicopter Vibration," *Journal of the American Helicopter Society,* Vol. 28, No. 3, July 1983, pp. 33-41.

[6]Friedmann, P. P. and Shanthakumaran, P., "Optimum Design of Rotor Blades for Vibration Reduction in Forward Flight," *Proceedings of the 39th Annual Forum of the American Helicopter Society,* St. Louis, MO, May 1983.

[7]Kottappalli, S. B. R., "Hub Loads Reduction by Modification of Blade Torsional Response," *Proceedings of the 39th Annual Forum of the American Helicopter Society,* 1983.

[8]Desjardins, R. A. and Hooper, W. E., "Helicopter Rotor Vibration Isolation," *Vertica,* Vol. 2, 1978, pp. 145–159.

[9]Braun, D., "Ground and Flight Tests of a Passive Rotor Isolation System for Helicopter Vibration Reduction," *Vertica,* Vol. 8, No. 1, 1984, pp. 1–14.

[10]Robert, J., "An Analytical and Model Test Research Study on the KAMAN Dynamic Antiresonant Vibration Isolation (DAVI)," U.S. Army Aviation Materiel Laboratories (USAAVLABS) Tech. Rept. 68-42, Nov. 1968.

[11]Wood, E. R., Powers, R. W., Cline, J. H., and Hammond, C. E., "On Developing and Flight Testing a Higher Harmonic Control System," *Proceedings of the 39th Annual Forum of the American Helicopter Society,* St. Louis, MO, May 1983.

[12]Molusis, J. A., Hammond, C. E., and Cline, J. H., "A Unified Approach to the Optimal Design of Adaptive and Gain Scheduled Controllers to Achieve Minimum Helicopter Rotor Vibration," *Journal of the American Helicopter Society,* Vol. 28, No. 2, April 1983, pp. 9–18.

[13]Davis, M. W., "Development and Evaluation of a Generic Active Helicopter Vibration Controller," *Proceedings of the 40th Annual Forum of the American Helicopter Society,* Arlington, VA, May 1984.

[14]Molusis, J. A., "The Importance of Non-linearity on the Higher Harmonic Control of Helicopter Vibration," *Proceedings of the 39th Annual Forum of the American Helicopter Society,* St. Louis, MO, May 1983.

[15]Daughaday, H. and McIntyre, H. H., "Suppression of Transmitted Harmonic Loads by Blade Pitch Control," *Proceedings of the 23rd Annual National Forum of the American Helicopter Society,* Washington, DC, May 1967.

[16]Prouty, R. W., "Aerodynamics," *Rotor and Wing International,* Vol. 18, Jan. 1984, pp. 14–18.

[17]Hohenemser, K. H. and Yin, S. K., "The Role of Rotor Impedance in the Vibration Analysis of Rotorcraft," *Vertica,* Vol. 3, 1979, pp. 189–204.

[18]Hsu, T. K. and Peters, D. A., "Coupled Rotor/Airframe Vibration Analysis by a Combined Harmonic Balance–Impedance Matching Method," *Journal of the American Helicopter Society,* Vol. 27, No. 1, Jan. 1982, pp. 25–34.

[19]Kunz, D. L., "A Non-linear Response Analysis and Solution Method for Rotorcraft Vibration," *Journal of the American Helicopter Society,* Vol. 28, No. 1, Jan. 1983, pp. 56–62.

[20]Stephens, W. B. and Peters, D. A., "Rotor-Body Coupling Revisited," *Journal of the American Helicopter Society,* Vol. 32, Jan. 1987, pp. 68–72.

[21]Venkatesan, C. and Friedmann, P., "Aeroelastic Effects in Multirotor Vehicles with Application to a Hybrid Heavy Lift System," NASA CR 3822, Aug. 1984.

[22]Sivaramakrishnan, R., "Prediction and Reduction of Vibration in Helicopters," M.Tech. Thesis, Indian Institute of Technology, Madras, India, 1987.

[23]Johnson, W., *Helicopter Theory,* Princeton University Press, NJ, 1980, pp. 126–128.

[24]Friedmann, P. P. and Kottappalli, S. B. R., "Rotor Blade Aeroelastic Stability and Response in Forward Flight," Paper 14, *Proceedings of Sixth European Rotorcraft and Powered Lift Aircraft Forum,* Sept. 1980, pp. 14.1–14.34.

[25]Urabe, M., "Galerkin's Procedure for Nonlinear Periodic Systems," *Archives of Rational Mechanics and Analysis,* Vol. 20, 1965, pp. 120–152.

[26]Hsu, C. S. and Cheng, W. H., "Steady-State Response of a Dynamical System Under Combined Parametric and Forcing Excitation," ASME Paper 73-WA/APM 10, 1973.